q-factor estimation for 3D log-house timber buildings via Finite Element analyses

Chiara Bedon[a,*], Giovanni Rinaldin[a], Massimo Fragiacomo[b], Salvatore Noé[a]

[a] University of Trieste, Department of Engineering and Architecture, Piazzale Europa 1, 34127 Trieste, Italy
[b] University of L'Aquila, Department of Civil, Construction-Architectural & Environmental Engineering, Via Giovanni Gronchi 18 - Zona industriale di Pile, 67100 L'Aquila, Italy

A R T I C L E I N F O

Keywords:
Log-house timber structures
Nonlinear dynamic analyses
Finite Element (FE) numerical investigation
Seismic performance
Experiments
Q-behaviour factor

A B S T R A C T

The paper numerically investigates the structural response of log-house (or log-haus, *Blockhaus*, etc.) timber buildings under seismic loads. The typical log-house system consists of a series of timber members, stacked horizontally one upon another. There, the mechanical interaction is given by traditional timber joints with carvings, multiple contact surfaces, friction phenomena. Even though log-house systems are widely used for the construction of wooden houses or commercial buildings in earthquake-prone regions, no design provisions are currently given in design standards. In this paper, a Finite Element (FE) numerical investigation is performed in ABAQUS on full three-dimensional (3D) log-house buildings subjected to seismic loads, as an extension of past studies focused on single components and walls only. In the typical FE model, the cyclic behaviour of carpentry joints at the interception between multiple logs and walls is properly accounted, including frictional effects and possible tolerance gaps due to the construction process. Nonlinear dynamic analyses are carried out on a set of selected building configurations of technical interest for design, giving evidence of their structural performance. Based on the so collected parametric FE results, estimations of the q-behaviour factor are hence discussed. As shown, the FE data suggests that - compared to other timber structures - a larger inter-storey drift should be considered for the seismic design of log-house buildings. In addition, the same FE results show that a q-behaviour factor up to 2.8 can be accounted.

1. Introduction

Despite the ancient origins, log-house timber structures are currently used for the construction of wooden houses and commercial buildings (see for example Fig. 1 [1]) that are at the design stage are frequently asked to resist severe seismic loads.

The timber walls are constructed by placing a series of simple logs, horizontally on the top of one another. These logs are often made of strength class C24 spruce according to [2], and typically have a cross-section with height h over width b (h/b) ratio in the range 1.6–2.4. Sometimes, the h/b ratio of the logs can be in the order of ≈ 0.8, while fully rounded logs (i.e. Fig. 2) are also available on the market. Small protrusions and tongues are finally used to increase interlocking between the overlapping timber members, with specific geometrical features and minor variations depending on the producer.

As a general intrinsic design concept, the mechanical interaction between the basic components is provided by simple mechanisms, such as carpentry joints (see for example Fig. 2(f) and (g)) and contact surfaces, while the use of metal fastener is reduced to a minimum. Metal fasteners are avoided also in presence of interrupted logs in the vicinity of door/window openings, aiming to allow free shrinkage settlement in the vertical direction of timber members, through the full design life of a given building. As a result, the openings themselves should be properly taken into account when assessing the overall structural behaviour of log-house systems, both at the component and assembly level. Additional steel stiffeners can be in fact used along the vertical edges of door/window openings (see for example [3,4]). However, these profiles are not rigidly connected to the adjacent logs, but kept in position by pressure contacts only. Consequently, the metal stiffeners provide limited contribution to the overall structural resistance of the building, especially in the case of log walls subjected to in-plane lateral loads and extreme design actions in general. Each log-house wall, finally, is usually connected to a reinforced concrete (RC) foundation slab by means of steel angular brackets, spaced at ≈ 1.5 m. Permanent gravity loads are transferred onto each main wall by the inter-storey floors. Depending on the type of assembly, the inter-storey

* Corresponding author.
E-mail address: chiara.bedon@dia.units.it (C. Bedon).

Accepted 29 September 2018

Fig. 1. Examples of log-house buildings (courtesy of Rubner Haus AG SpA [1]).

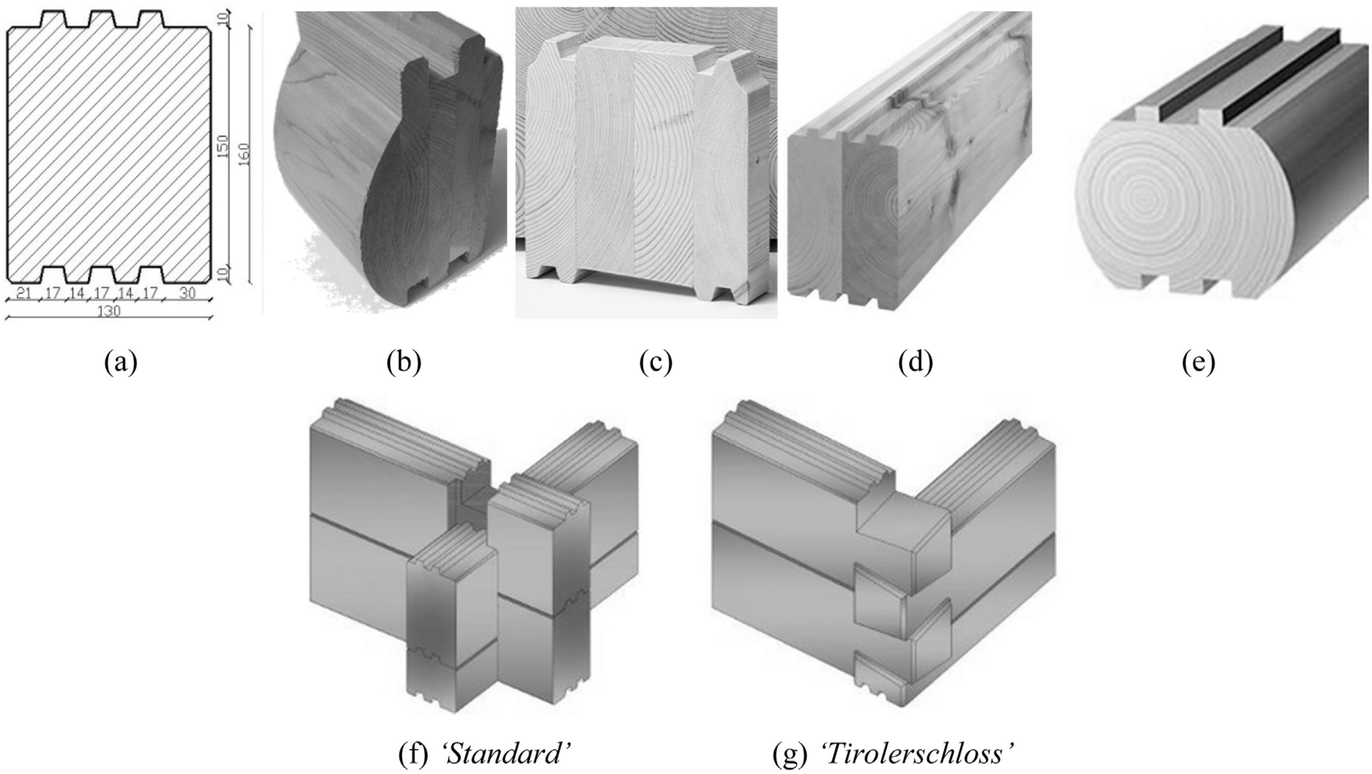

Fig. 2. Examples of cross-sections ((a) to (e)) and corner joints (f, g) currently available on the market for log-house buildings. Reference geometrical features taken from: (a, f, g) www.rubnerhaus.com (with nominal dimensions given in cm); (b): www.linclonlogs.com; (c): www.polarlifehaus.com; (d): www.eurowood.co.nz; (e): www.satterwhite-log-homes.com.

floors can also provide an in-plane rigid diaphragm, hence resulting in a further lateral restraint able to avoid possible local deformations or out-of-plane deflections of the top logs of each wall. Such an in-plane rigid floor diaphragm can be achieved by using either Oriented Strand Board (OSB) panels, timber joists and blocking, with the OSB sheathing properly nailed along the entire perimeter, or glulam panels arranged on their edges with proper connection between adjacent panels, see also [5]. From a design point of view, the currently available standards for timber structures (i.e. [6,7]) do not provide analytical models and recommendations for an appropriate verification of log-house structural systems, either under ordinary design actions or exceptional loads such as seismic events.

1.1. Past research studies

Few contributions can be found in the literature about the structural behaviour of log-house systems, under various loading configurations of interest for design.

Part of these studies are related to buckling (see [4,5,8]) or fire resistance issues [9,10].

Some researchers also investigated – via experimental tests, analytical models and/or FE analyses – the mechanical characterization of single log-house structural components, or single walls belonging to full 3D assemblies. Scott et al. [11,12] investigated experimentally and numerically the in-plane seismic response of walls composed of round logs, with careful consideration for the anchoring systems. The structural efficiency of trough-rods was verified, providing evidence of the crucial role played by friction phenomena in the overall shear response of such assemblies. Single log-walls have been experimentally investigated also in [13–16], under the effects of monotonic and/or cyclic in-plane lateral loads, including variations in the imposed vertical compression ratio as well as variations in geometrical configuration for walls and log components/joints. In [17], the in-plane response of corner joints in use for log-house systems was investigated via refined 3D solid models, giving evidence of their typical response in the elastic and damaged phases, as a function of variations in the loading conditions.

The seismic performance of three dimensional log-house buildings has been investigated by means of full-scale experimental shake table tests [18,19], including some simplified FE numerical simulations [20]. Generally, the series of full-scale shake table tests reported in [18,19] gave evidence of the high flexibility of log-house systems. This experimental finding was further proved in [21], where structural and non-structural damage scenarios observed in several existing log-houses, after the 2016 New Zealand earthquake, were discussed.

1.2. Aim of the work and methods

Within the available seismic design recommendations for buildings (i.e. the Eurocode 8 [7]), a key role is conventionally assigned to the reference value for the q-behaviour factor of a given structural system, being such a value representative of its actual energy dissipation capacity (q ≥ 1 for dissipative systems). Despite the promising experimental observations and the good performances of real buildings under seismic loads [18,19,21], a design issue for log-house systems is represented by the lack of accurate provisions for the estimation of their behaviour factor. As a log-house system is in fact expected to not dissipate significant amount of energy, the q-factor should lay in the order of 1.5 [19]. However, typical friction phenomena at the interface of logs in contact are conventionally estimated in q = 2 (see for example [19,22]).

In this regard, aiming to fill the gaps of current design recommendations for log-house timber structures, a preliminary numerical estimation of the expected q-factor for single log-walls under in-plane seismic loads has been proposed in [23]. The numerical research study was based on a FE model previously developed (see [3,24]) and validated towards earlier experiments.

In this paper, the FE modelling approach presented in [23] for single walls is further extended and used to investigate the seismic performance of full 3D log-house buildings. The novel aspect of this research study is represented by nonlinear dynamic analyses carried out in ABAQUS [25] on three-dimensional buildings, rather than on single walls, thus including both in-plane and out-of-plane phenomena in the so estimated global q-factor. To this aim, the typical 3D FE model is first validated towards experimental shaking table test results derived from [18,19] for a two-storey log-house building, including comparisons with the available modal identification measurements. The FE model is then used to assess the seismic performance of three case study buildings ('B01′, 'B02′ and 'B03′, in the following) representative of design configurations of technical interest (i.e., actual buildings constructed in seismic regions of Italy). The most important results of the nonlinear dynamic simulations are hence presented, providing evidence of the effects due to some key input parameters, such as (i) the geometrical features of the corner joints, (ii) the presence and amplitude of gaps at the interface between the orthogonal logs (production tolerances), and (iii) the in-plane flexibility of inter-storey floors. Finally, estimations for the q-factor of log-house buildings are also proposed and critically discussed. In doing so, two different approaches for the definition of the reference configurations - and the related effects on calculations - are also emphasized, especially with respect to the yielding state. The high dissipative capacity of log-house systems is hence highlighted.

2. Nonlinear dynamic analysis of 3D log-house systems

2.1. General FE modelling approach

Full 3D log-house buildings are investigated in this paper using the same FE modelling approach reported in [3,23,24], with appropriate modifications, so to account for spatial assemblies rather than single walls under in-plane lateral loads. In general terms, each single log-wall can be first described, by means of a series of overlapping rigid beams. In accordance with Fig. 3(a), these beams are connected at their ends by means of nonlinear spring elements, acting in their axial (Y direction) and transversal (shear – X and Z directions) degrees of freedom. A single spring, in this context, aims to reproduce the actual cyclic behaviour of a carpentry joint agreeing with Fig. 2(f) and (g), with careful consideration for the joint resistance to shear (i.e., sliding in X and Z directions) and for the compressive forces (Y direction) applied on one-half of each log. The advantage of such a FE modelling approach is that the presence of door and/or window openings can be also taken into account, see [3,23]. There, the structural discontinuity of logs can in fact be considered, hence local collapse mechanisms due to in-plane lateral loads are reproduced. At the same time, the shear resistance ($V_{profile}$) of possible metal profiles along the vertical edges of openings can be accounted. The final result is that possible relative sliding phenomena and out-of-plane displacements of each timber log are neglected as far as the given $V_{profile}$ resistance is not exceeded. Once multiple log-walls are assembled together, 3D geometrical configurations of realbuildings can hence be investigated.

2.1.1. FE modelling concept and springs calibration

In the current FE study, a single type of 'Standard' carpentry joints was first considered for the parametric analyses, see Fig. 2(f) and Table 1, where the joint is detected as 'N01′ type, based on [3,23]. The calibration of each spring was hence derived from past efforts, including test data and numerical simulations on single log-house walls [3,23].

More in detail, the axial law of Fig. 3(b) was used to represent the contact behaviour in compression between the overlapping timber logs in a lumped way, while the shear law is symmetric (Fig. 3(c)). In the first case (branch #10 of Fig. 3(b)), the compressive resistance was estimated by multiplying the characteristic compressive strength $f_{c,90,k}$ of C24-class timber (in the direction perpendicular to the grain) by the top/bottom contact surface of a single log. The tensile response of each spring, on the other hand (branch #1 of Fig. 3(b)), was described in the form of an almost null stiffness, so as to represent the possible uplift and separation of one timber beam from another. The shear hysteretic law of Fig. 3(c), separately applied for two in-plane shear directions, is characterized by a tri-linear backbone curve and specific unloading-reloading paths from the elastic (i.e., before F_{el}, in Fig. 3(c); see the branches #1 and #10 on the backbone curve) and the inelastic phases (branches #2, #3, #20 and #30 on the backbone curve). The unloading paths in the elastic phase, displayed in Fig. 3(c) with dashed lines, are then characterized by two branches: the first one (branch #11) leads to a null strength with a stiffness k_{sc} times the elastic one (see also Table 1), whereas the latter one (branch #12) leads to a percentage of the maximum displacement reached on branch #10. The reloading path in Fig. 3(c) in the elastic phase, finally, is symmetric compared to the unloading path (branches #110 and #120). The unloading and reloading paths are composed by four branches each (#4, #8, #6, #40 and the symmetric ones), which schematize the pinching effect in the plastic phase, for unloading starting from branches #2 or #3, and #20 or #30. The branch #4 has a stiffness k_{sc} times the elastic term, while the slope of branch #8 is a fraction of the elastic one. The branches #40 and #5 are finally characterized by a degrading elastic stiffness. Such a degradation is linear and starts once F_{el} is attained; the ultimate value is used at the ultimate displacement and is equal to k_{deg} times the elastic stiffness. The spring law implements also a strength degradation through an additional displacement at reloading (δ_E in Fig. 3(c)), which is proportional to the dissipated energy in the last full reversed cycle and can be described by means of the parameters α and γ (Table 1).

The effect of dynamic friction is also included in the typical 3D FE-model (Fig. 3(d)), since it provides an additional strength contribution to each shear spring given by:

$$F_f = C_f \cdot N, \tag{1}$$

where N signifies the resultant axial (vertical) force in the spring at the current analysis step, while C_f and F_f denote the dynamic friction coefficient and the dynamic friction force in the shear direction of the spring. In this study, the stiffness term k_f (Fig. 3(d)), was set equal to 10

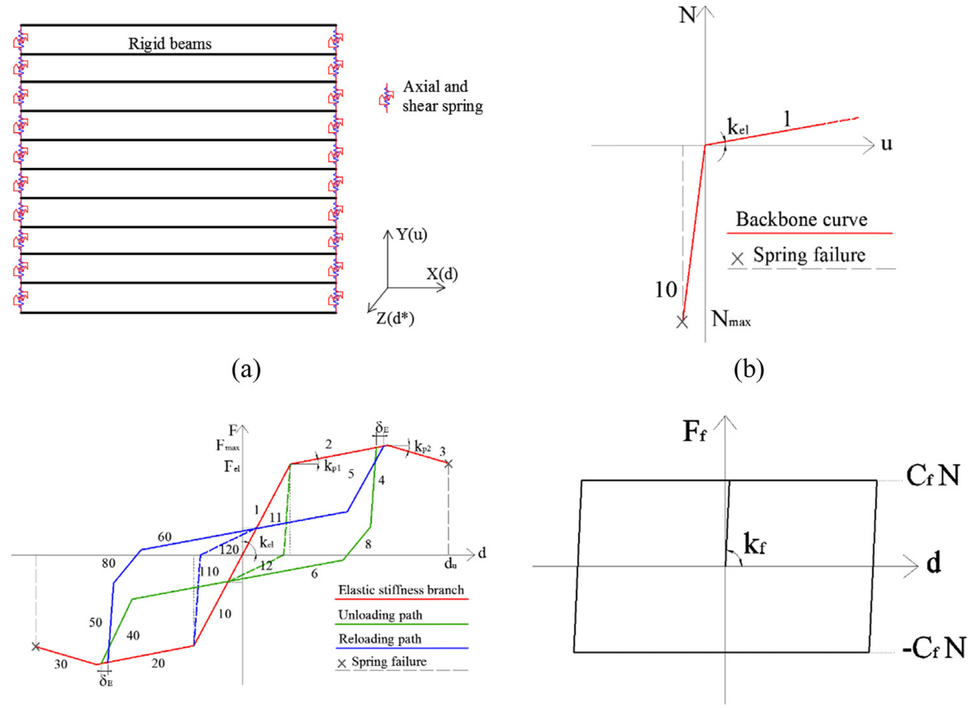

Fig. 3. FE assembly of the typical log-house system. (a) Schematic view of a single log-wall, with constitutive laws in springs representative of (b) axial DOF, (c) shear DOFs and (d) friction.

Table 1
Calibration of the input parameters for the FE modelling of full 3D log-house buildings, according to [3,23].

Parameter symbol	Calibrated value	Units	Reference cyclic behaviour
k_{el}	3.34	kN/mm	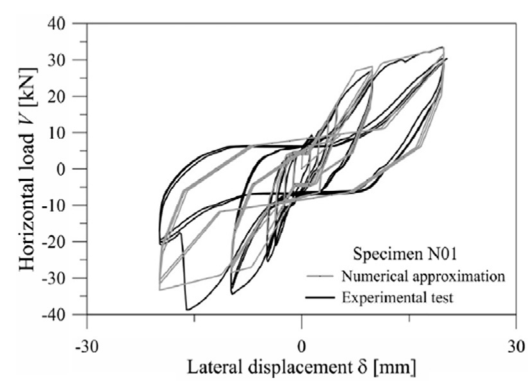
F_{el}	23.01	kN	
k_{p1}	0.49	kN/mm	
F_{max}	33.51	kN	
k_{p2}	− 1.47	kN/mm	
k_{sc}	1.5	–	
R_C	0.6	–	
S_C	0.65	–	
d_u	20	mm	
k_{deg}	0.6	–	
α	1	–	
γ	0.0003	–	
gap	1	mm	
k_5	1.2	–	

times the shear stiffness of the connector (branch #1 in Fig. 3(c)). Based on [3,23], C_f was assumed equal to 0.4 for the full parametric study.

2.1.2. FE assembly of 3D log-house buildings

In this paper, the typical 3D log-haus building was numerically described as an evolution of single log-walls analyzed in [3,23]. As briefly recalled in Section 2.1.1, each one of the springs of Fig. 3 was implemented to return to the solver three stiffness terms only (i.e., one for the axial DOF and two for shear DOFs), so as to cover all the translational DOFs of a given carpentry joint. When assembling full 3D assemblies composed of multiple intercepting log-walls, rotational DOFs were indeed neglected, due also to the lack of experimental results of literature to support any kind of calibration. An additional high-stiffness linear spring was in fact used at the end/interception of each log, so as to restrain the torsional DOF of the rigid beams representative of timber members. Beam elements (B31 type) with simplified $b \times h$ cross-section were in fact used to describe the timber logs. In doing so, following earlier numerical studies (i.e. [5,8]), possible contributions of the typical tongues and grooves characterizing the cross-section of logs (see Fig. 2) were rationally neglected. Given a set of springs and rigid beams herein described, the hypotasis of the so-assembled 3D FE models was hence ensured. The inter-storey floors and roofs, in addition, were described via kinematic constraints, and accounted in presence of fully rigid in-plane diaphragms only. Additional lumped masses representative of the structural self-weight of each 3D assembly were finally applied to the centre of gravity of the storey levels, while vertical loads acting on the building were uniformly distributed on the top logs only.

2.2. Validation of the 3D FE modelling approach

A first validation of the FE modelling approach described in Section

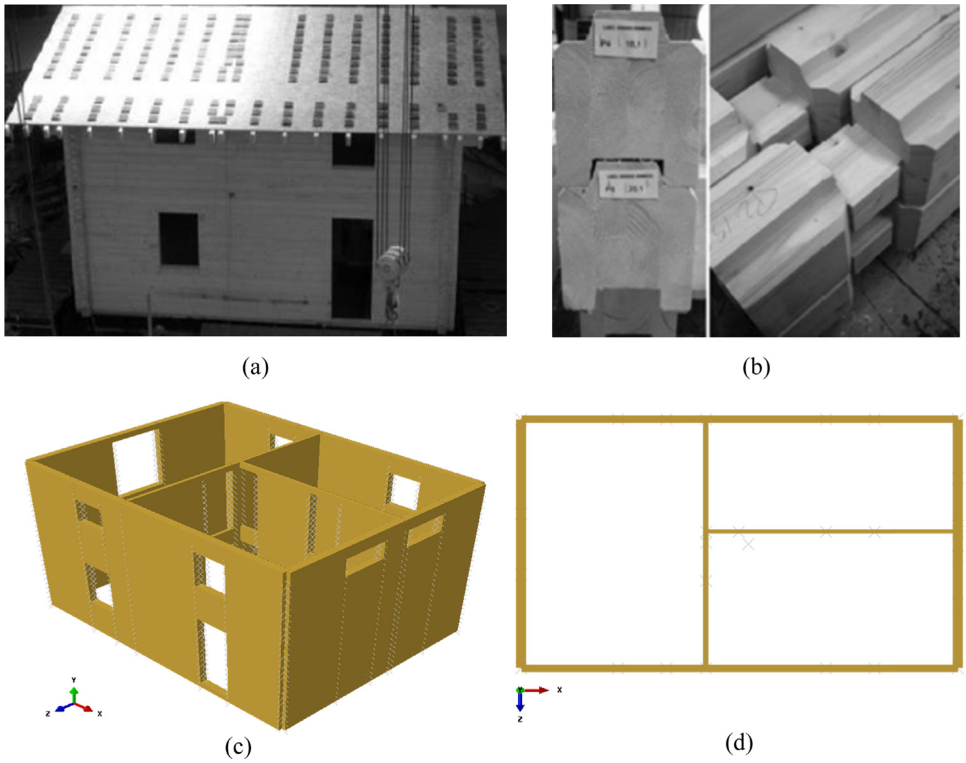

Fig. 4. FE modelling of the ‘Rusticasa building’. (a) Overview of the experimental full-scale specimen and (b) detail of timber logs [18,19], with (c) extruded 3D and (d) plan views of the corresponding FE model (ABAQUS).

2.1 was carried out, so as to assess its potential when extended to full 3D timber log structures. To this aim, full-scale test results available in the literature were taken into account, and special care was spent for the ‘Rusticasa building’, the dynamic and seismic performance of which has been experimentally investigated within the framework of the SERIES Timber building project (see Fig. 4(a) and [18,19]). The reference ‘Rusticasa building’ reported in [18,19] and numerically reproduced herein for qualitative comparisons is a two-storey log-house assembly, characterized by a 5.64 × 7.30 m rectangular plan, a total height of 4.40 m at the edge of the gable roof and a total height of 5.28 m at the ridge. The building, see Fig. 4(a), is almost symmetric along the longitudinal direction, and asymmetric in the transversal direction. At the time of the full-scale shake table experimental investigation, the 3D sample was assembled in the form of log-walls composed of 160 × 160 mm and 80 × 160 mm logs (C24 class spruce), in use for the perimetral and the internal walls respectively.

22 mm thick, OSB sheathing panels supported by timber joists were used to ensure an in-plane rigid inter-storey floor to the building. Moreover, 398 additional steel plates (7.1 kg/each) were equally distributed on the roof, to act as permanent loads during the experiments. A full description of the Rusticasa building geometry, including test methods and results, can be found in [18,19].

2.2.1. Modal analysis

According to Section 2.1, the 3D FE model of the ‘Rusticasa building’ (see Fig. 4(c) and (d)) was first implemented in ABAQUS. The in-plane rigid, inter-storey floor was modelled via a kinematic constraint, while the dead loads (self-weight of the structural members and additional permanent loads) were applied - as nodal masses - in the centre of gravity of the first floor and the roof. The 398 additional steel plates were also lumped in the centre of gravity of the roof, so as to reproduce the experimental sample [18,19]. In terms of mechanical characterization of the carpentry joints at the interception of logs, finally, the input parameters corresponding to the ‘N01′ joint summarized in Table 1 were used.

The eigenvalue analysis was carried out on the so calibrated 3D assembly, in order to predict the fundamental vibration modes of the building and compare them with the corresponding experimental estimations, as obtained in [18,19] via dynamic identification techniques. To this aim, the modal test measurements available in [18] for the ‘Rusticasa building’ before the execution of the set of shaking table tests were considered. IMultiple modal dynamic calculations were in fact carried out on the same building (up to seven repetitions, in total), at the end of each seismic experiment, so as to assess via dynamic identification techniques the occurrence of possible damage due to shake table tests. However, the dynamic estimations generally resulted in null or minor structural damage in the main specimen components, as confirmed by limited variations in the calculated natural vibration periods.

Even though in low-rise buildings the seismic performance is mainly related to the first vibration period and shape, four vibration modes were numerically detected in this study, and compared with the experimental estimations reported in [18,19].

The test measurements summarized in [18,19] for the ‘Rusticasa building’ revealed, in particular, the presence of a mainly longitudinal fundamental modal shape, but inclusive also of certain transversal displacement components. During the full series of modal dynamic experiments discussed in [18,19], such a kind of mixed deformation proved to be an intrinsic feature of the examined log-house system, due to discontinuity of timber walls and to the reciprocal interaction between multiple timber members, based on carpentry joints and interceptions mechanisms. The same feature, consequently, resulted in a rather difficult/ambiguous classification of modal shapes. A mixed translational shape was in fact experimentally derived also for the second vibration mode of the ‘Rusticasa building’, while mainly torsional shapes were detected for third and fourth modes.

Despite the intrinsic uncertainties in the geometrical and mechanical description of the reference 3D assembly, as well as in the availability of single test measurements only, a rather good correlation was observed between the past modal predictions derived from [18,19] and

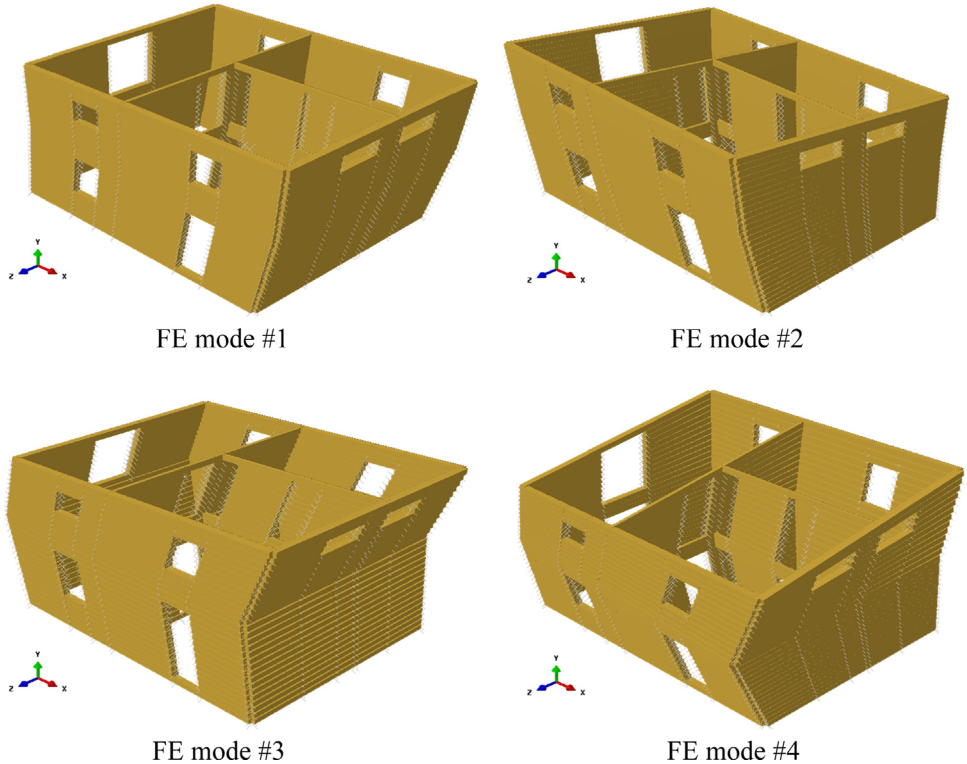

Fig. 5. Numerically predicted fundamental vibration shapes for the 'Rusticasa building' (ABAQUS).

Table 2
Experimental [18,19] and numerical (ABAQUS) vibration frequencies for the Rusticasa building. Key: $\Delta_f = 100 \times ((f_{exp} - f_{num})/f_{num})$.

Vibration Mode #	Frequency [Hz]		Δ_f
	Experimental	FE	[%]
1	5.38	5.39	− 0.19
2	11.85	10.55	12.32
3	14.93	14.80	0.88
4	20.53	28.62	− 28.27

the numerical estimations collected herein for the full 3D FE assembly. Fig. 5, in this regard, shows the FE normalized vibration shapes of the first predicted vibration modes, while Table 2 collects the corresponding frequencies, together with the past experimental values and the corresponding percentage scatter. Worth of interest, see Fig. 5, is that the first FE vibration shape calculated in ABAQUS revealed the presence of a mainly longitudinal mode for the 3D assembly, that is in agreement with preliminary elastic calculations from [18,19]. Despite the simplifications of the FE modelling approach, a fairly good correlation was found also for the higher modes of the building, between numerical and experimental vibration shapes of Fig. 5 and the corresponding frequencies, see Table 2. A large discrepancy, up to −28% of the experimental frequency, was obtained only for the fourth mode only, which proved to be highly affected by torsional components of deformation. Such an outcome remarks the dynamic complexity of the examined building (i.e., due to contacts, gaps, imperfections, etc.) but also suggests the reliability of the implemented FE model, in particular with respect to the fundamental vibration mode, which is the most relevant for seismic analyses.

2.2.2. Seismic analysis

The 3D numerical model of the 'Rusticasa building' was successively investigated by means of nonlinear dynamic simulations, in order to globally assess its seismic performance and further verify the reliability of the proposed FE model for seismic purposes. In accordance with [18,19], the 1979 Montenegro earthquake record was considered as seismic input for the 3D assembly of Fig. 4.

The full set of past experiments reported in [18,19], in particular, included multiple tests on the same building, with shake test repetitions carried out to assess the effects of several scaled Montenegro records, with PGA values in the range of 0.07–0.5 g. In this research study, a set of dynamic simulations was hence carried out by taking into account several amplitudes for the assigned seismic record, i.e. by first subjecting the FE model to a low intensity earthquake (PGA = 0.07 g), then to a moderate (0.28 g) and finally to a high intensity earthquake (up to 0.35 g, in the current numerical investigation).

The typical deformed shape of the 3D FE assembly under seismic records is shown in Fig. 6, as obtained for an assigned input of PGA = 0.28 g.

Given such a kind of numerical outcomes for the reference 3D model, the qualitative assessment of dynamic FE predictions towards the past shaking table tests was carried out by comparing the numerical and experimental displacement measurements for selected control points. In addition, a qualitative comparison of possible damage scenarios was also performed. In accordance with main purposes of the current research study, in particular, a maximum seismic PGA up to 0.35 g was considered for the parametric numerical analyses, as this is the higher values prescribed by standards in use for the seismic design of buildings [7]. For the selected PGA = 0.28 g scenario of Fig. 6, for example, no structural damage was noticed, either in the full-scale specimen [18,19] or in the simplified FE model presented herein. In the past SERIES experiments, more in detail, minor damage was noticed only at the end of the full set of shake table tests, that is for scaled Montenegro seismic records corresponding to a PGA = 0.5 g input. In addition, such a detected damage proved to be limited to minimum regions of the building, and was mostly revealed by variations of the measured frequencies and visual observations (i.e. relative sliding of logs due to shear - especially close to door/window openings - and fracture of logs along the grains). In the case of the current 3D numerical simulations, based on the FE assumptions earlier described, the

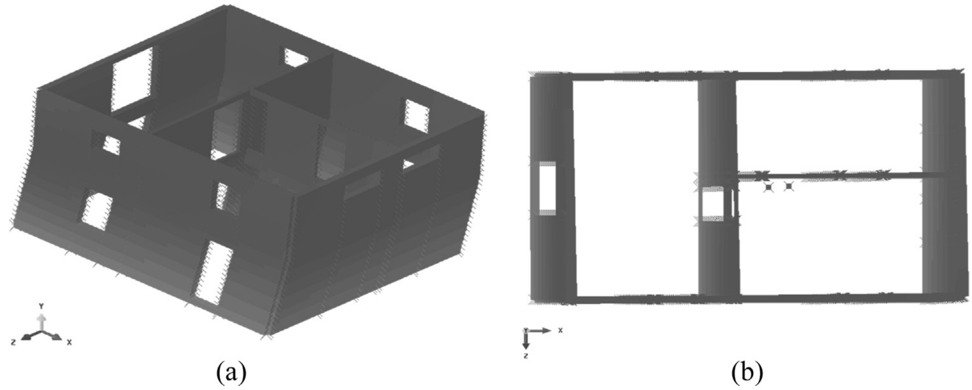

Fig. 6. Typical deformed configuration of the ‘Rusticasa building’ FE-model under the 1979 Montenegro seismic record (0.28 g), scale factor: 500). (a) Extruded 3D view and (b) top view (ABAQUS).

occurrence of possible failure mechanisms was accounted and eventually detected by monitoring the occurrence and evolution of possible plastic phenomena in the overall cyclic response of each carpentry joint. From the same FE predictions, the average maximum sliding in carpentry joints due to a PGA = 0.28 g seismic input was found to be about 0.5 mm, hence largely comprised within the assigned tolerance gap (see Table 1) and excluding the occurrence of possible failure mechanisms in them.

In terms of numerical and experimental comparisons for a given loading scenario, a rather close qualitative agreement was found also in terms of measured drifts for the ‘Rusticasa building’, despite the intrinsic simplification of the FE model and the experimental uncertainties due to limited test data/repetitions. For the seismic record corresponding to the deformed shape displayed in Fig. 6, for example, the maximum experimental drift at the ground floor was found equal to 0.005 [18,19], while the corresponding FE estimation obtained herein was 0.004. At the first inter-storey level, the maximum drift was in the order of 0.003 for the full-scale experimental test and 0.002 for the simplified 3D FE model.

For the examined range of seismic records (0.07–0.35 g), a mostly linear PGA-to-drift relationship was numerically observed, with ≈ 0.007 the ground floor drift for 0.35 g. Since the intrinsic features of log-house buildings under lateral loads typically manifest in a top displacement that is given by the sum of cumulative sliding effects in each carpentry joints (with 16–18 the typical number of stacked logs for each inter-storey level, see also [3,17]), even under extreme design loads, each joint is mostly required to suffer limited deformations. The general outcome of the drift measurements herein recalled for the ‘Rusticasa building’, for example, can be expressed in a single joint sliding in the range of 0.5–1 mm (as derived from both the past experimental measurements and the current FE estimations).

3. Parametric study on real 3D log-house systems

An exploratory FE study was hence carried out by taking into account several log-house building configurations. The same modelling approach validated in Section 2 was taken into account. To this aim, in particular, geometrical features representative of real log-house systems constructed in Italy were considered [1].

3.1. Selected case studies

In this paper, a selection of case study buildings is reported and discussed in detail, so as to point out the typical dynamic response of log-house assemblies. Fig. 7 shows the undeformed geometrical configuration for the 3D buildings presented in the paper. The building selection aimed at explore the effects of some key structural features, including variations in the log/building size, plan configuration, openings, etc.

The first case study (‘B01′, in the following, see Fig. 7(a)) represents a single storey log-house system, with 4.90 × 7.10 m regular plan and 2.50 m height (4.60 m at the ridge). The walls are made of 200 × 200 mm, C24 class resistance spruce logs. The openings consists in a single door (on the short side of the building), and four small windows (two on each side, symmetrically aligned on the longest walls). The second example (‘B02′, Fig. 7(b)) is a single storey log-house building characterized by a symmetric configuration along both the longitudinal and the transversal directions. The plan of the 3D assembly has almost a square shape, with 9.40 × 10.15 m dimensions and 2.66 m the height of the building at the edge of the roof (4.10 mm at the ridge). In this case, the log-walls have rectangular 80 × 190 mm section, with C24 class resistance spruce logs. Doors and window openings are mostly symmetrically distributed on the internal and external walls.

The third examined building (‘B03′, Fig. 7(c)), finally, is a single storey system characterized by a markedly asymmetrical geometrical configuration. The plan has overall dimensions of 9.70 × 11.80 m, while the building height is 2.48 m (4.10 m at the roof edge). The log-walls are composed of 90 × 160 mm, C24 class spruce logs. Together with an overall asymmetrical configuration for the building, a random distribution in door and window openings can be also noticed in Fig. 7(c), hence resulting in potential decrease of the overall seismic resistance for the examined system, as a major effect of its marked structural irregularity.

3.2. Seismic performance

The B01-to-B03 buildings were preliminary analyzed via eigenvalue simulations, so as to explore their dynamic performance and estimate the corresponding fundamental vibration modes. Fig. 8 shows the so predicted vibration shapes. The corresponding frequencies were found to be 9.95 Hz, 9.92 Hz and 11.12 Hz respectively.

In order to assess more in detail the structural performances under severe seismic events, each 3D building was hence further investigated via nonlinear dynamic analyses, by imposing a set of seven spectrum compatible natural seismic accelerograms obtained from REXEL v.3.5 software (www.reluis.it, [26]). In accordance with design standards in use for buildings, all the earthquake records were derived by considering a PGA of 0.35 g, with type A soil (e.g. rock soil), topographic category T1 and nominal life of 50 years. A maximum lower and upper tolerance of 10% was considered in the derivation of the seven natural seismic records, see Fig. 9(a).

The assessment of the seismic performance of the B01 to B03 systems was carried out by monitoring the maximum inter-storey drifts and the cyclic response of each carpentry joint. A qualitative assessment of the obtained FE results was also carried out in terms of global deformed shape and occurrence of possible local mechanisms, especially

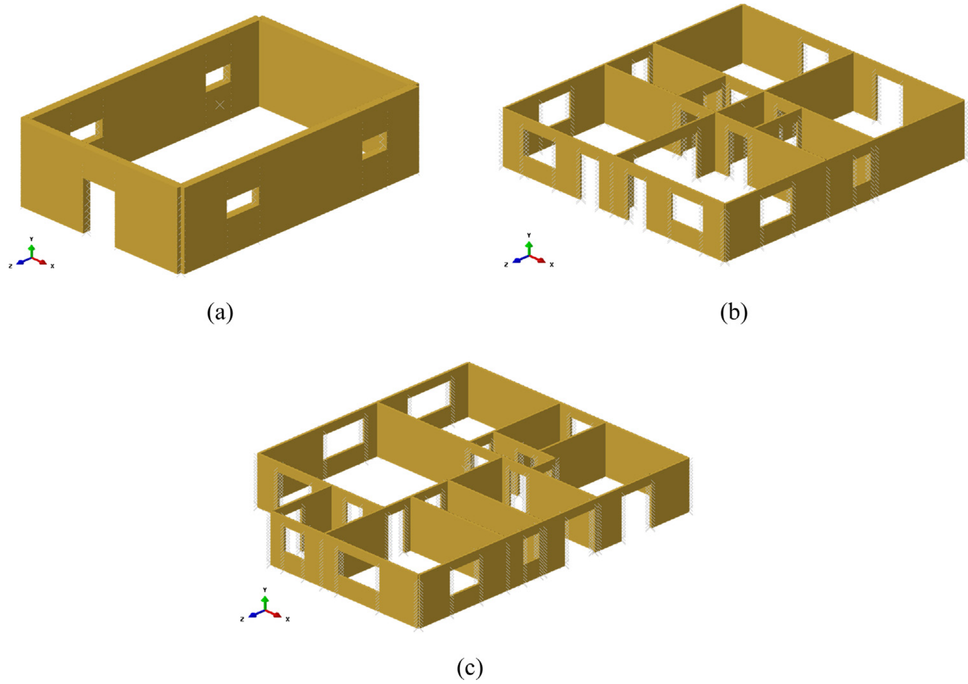

Fig. 7. 3D models of the log-house buildings investigated through the parametric study (extruded 3D view, ABAQUS). Case studies labelled as (a) 'B01', (b) 'B02' and (c) 'B03' buildings.

near the door/window openings and at the intersection between orthogonal log-walls.

In general, in accordance with [3,23], the investigated buildings highlighted a marked flexibility under the assigned seismic records, due to local deformations occurring at the level of each carpentry joint. As expected, however, even in the presence of tolerance gaps at the interface between the intercepting logs, the seismic performance of 3D assemblies was generally found to be enhanced, with respect to the behaviour of single log-walls under in-plane lateral loads (see [3,23]). Such a finding confirms the need of accurate investigations at the building level, rather than on single components only, when assessing the seismic behaviour of log-house buildings. At the same time, it remarks the potential of numerical methods, in support of time/cost consuming full-scale experimental tests.

Table 3 collects some selected FE comparative results, as obtained for the selected log-house systems.

The maximum obtained drift ratios were found equal to ≈ 0.0015, corresponding to a top displacement of 3–4 mm, hence in the same order of the 'Rusticasa building' FE model and the corresponding SERIES specimen (see Section 2). Regarding the single carpentry joints, a total maximum sliding in the order of 0.7 mm was obtained in each one of them. The effect of such deformations, given the input parameters collected in Table 1, can be hence quantified in a mostly frictional performance of the joints, being the so estimated sliding

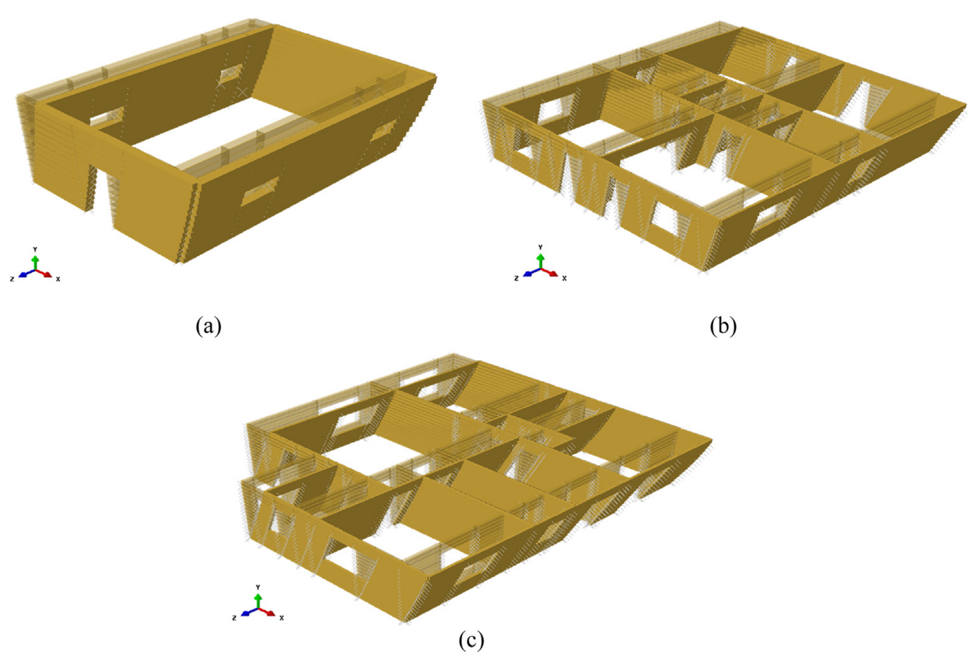

Fig. 8. Fundamental vibration modes for the (a) B01, (b) B02 and (c) B03 buildings (extruded 3D view, ABAQUS).

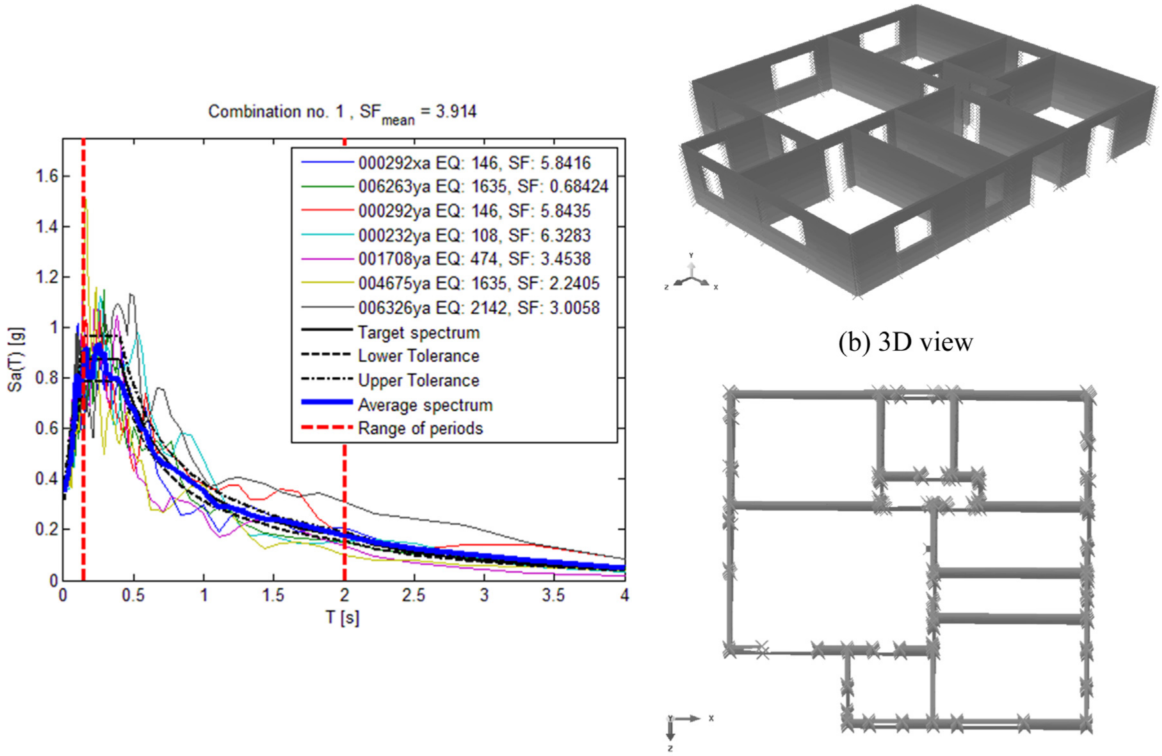

(a) (c) Top view

Fig. 9. (a) Reference set of natural seismic records obtained from REXEL v.3.5, with (b)-(c) typical deformed configuration of the B03 building under seismic events (0.35 g), scale factor: 5000, ABAQUS).

Table 3
FE comparative study (ABAQUS) on the dynamic performance of 3D log-house buildings under seismic events (0.35 g).

FE model#	Maximum drift ratio [-]		Maximum joint sliding [mm]
	x-dir.	*z-dir.*	
B01	0.0015	0.0005	0.708
B02	0.0010	0.0007	0.531
B03	0.0014	0.0011	0.525

amplitudes slightly higher than the assigned tolerance gap (with 1 mm the reference value, in the current investigation). In terms of overall performance and deformation of the same 3D assemblies, finally, a rather stable global behaviour was generally observed, even in the B03 building characterized by a markedly irregular geometry and by a large number of door and window openings (see for example Fig. 9(b) and (c)). No local failures were in fact observed, even in presence of structural discontinuities in the vicinity of interrupted logs. The presence of internal log-walls acting as partial bracing systems, in this context, typically resulted in a further increase of stability for the examined buildings, hence in an improved seismic performance for all of them.

3.3. Assessment of the most influencing parameters

Given the general agreement between the parametric dynamic estimations of Section 3.2, the B01 case study was then further investigated under the PGA = 0.35 g seismic records defined in Fig. 9(a), so that the effects of some key influencing parameters could be pointed out, for global and local structural assessment purposes.

Based on the main features and assembly method for the examined structural typology, careful consideration was given to the possible effects deriving from variations in (i) geometrical properties of the carpentry joints (see Section 3.3.1), (ii) amplitude of joint gaps due to production tolerances (Section 3.3.2), (iii) friction phenomena (Section 3.3.3), and (iv) in-plane flexibility of the inter-storey floors (Section 3.3.4).

3.3.1. Carpentry joints

The seismic performance of the B01 system assembled via different carpentry joint typologies was first investigated. Compared to the FE assumption of Section 2, the difference was represented by the input cyclic behaviour of springs, being the N01 ‘Standard’ joints replaced by ‘Tirol’ joints agreeing with Fig. 2(g). To this aim, the mechanical calibration of input parameters was taken from [3,23], where several joint samples and single walls were experimentally and numerically analyzed. For the sake of clarity, the geometrical and mechanical features for the so called ‘N03’ type joint under in-plane cyclic loads are recalled in Fig. 10. In the current FE investigation, it must be also pointed out that the use of ‘N02’ Standard joints described in [3,23] - i.e. with similar shape but differing in size details, compared to the N01 joints - generally led to minimum variations in the 3D dynamic estimations, due to the high similarity of N01 and N02 samples.

When the ‘Tirol’ joint N03 was used as a reference for the B01 case study, still limited variations were observed in terms of global and local seismic response, i.e. in terms of monitored maximum drifts and qualitative observations under the assigned set of seismic records (PGA = 0.35 g).

Such an outcome can be reasonably justified by the occurrence – as pointed out by the performed nonlinear dynamic simulations (see also Table 3) – of limited deformations at the level of each joint, typically lying in the order of ≈ 0.5 mm (with 1 mm the reference gap amplitude, see Table 1). As such, an almost pure frictional behaviour of the joints themselves was typically observed for all of them.

3.3.2. Joint gap amplitude

The effect of joint gaps with different amplitudes was then assessed,

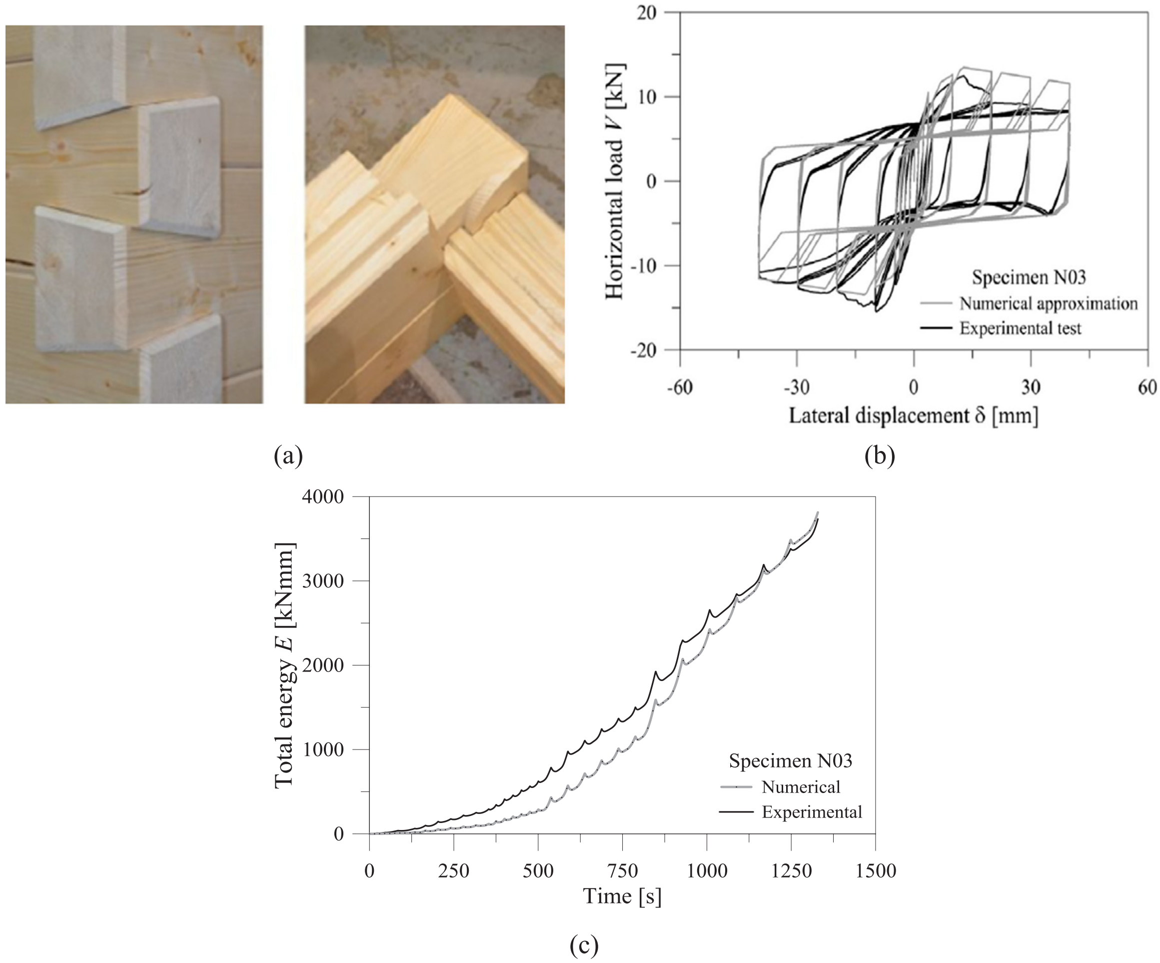

Fig. 10. 'Tirol' carpentry joint ('N03' type, in accordance with [3,23]). (a) Geometrical configuration and (b) FE calibration of its load-displacement cyclic behaviour, with (c) corresponding numerically and experimentally derived energies.

for the mechanical characterization of the N01 type springs. Such an assumption reasonably accounted for intrinsic uncertainties due to production tolerances and construction stages, see also [16,17]. Based on the average value of 1 mm provided in Table 1 and further validated in [3,23], in particular, the reference gap amplitude was progressively increased, up to a maximum value of 3 mm (1.5 mm, 2 mm and 2.5 mm the intermediate values), as well as reduced to a minimum of 0.5 mm. Such a set of gap amplitudes and the related parametric FE analyses was considered sufficiently wide to provide a rational feedback on possible gap-related effects (with 1.5 mm the expected nominal value), being 2 mm the gap amplitude experimentally measured in [16,17] for the same log typology.

For the B01 system under seismic records, the imposed gap amplitudes proved to have negligible effects on the overall dynamic performance of the 3D building (see some selected comparative results in Fig. 11(a)). This effect, as expected, was found to mainly derive from the interlocking between orthogonal logs, and to take advantage from the actual stiffening contribution due to in-plane rigid inter-storey diaphragms.

Major variations for the 3D assembly were observed especially with respect to the numerical outcomes reported in [16,17] for single carpentry joints, as well as to the FE/experimental findings provided in [3,23] for single log-house walls under in-plane seismic loads. In both the cases, the lack of lateral restraints for small-scale components and single walls (as it is within full spatial buildings) typically manifested in a marked sensitivity of seismic estimations to the imposed gap amplitudes. The current 3D FE outcomes, as a result, further confirmed the importance of performing seismic vulnerability investigations at the full assembly level, especially with the support of large-scale experimental background.

3.3.3. *Dynamic friction coefficient*

Following the spring calibration summarized in Section 2.1.1 for the N01 joints, the effects of variations in the dynamic friction coefficient C_f were also investigated. To this aim, the reference value of 0.4 was decreased to 0.3, in accordance with the experimental derivations provided in [16] for the same structural sample. Despite the marked variations in the assumed friction input parameter and according to Section 3.3.2, rather negligible variations were observed for the B01 system under the given set of seismic records (with PGA = 0.35 g), see Fig. 11(b). Such a finding still reflects the need of investigations at the assembly level, with respect to small-scale studies that could partly overestimate certain local phenomena, or whose reliability is strictly related to the appropriate description of actual boundaries (see for example [16,17]). Again, a key role was played by the presence in the B01 system of a fully rigid inter-storey floor, which is able to offer a rather stable global behaviour to the examined structural system, especially with respect to the limitation of possible sliding phenomena of logs (at their interception with the orthogonal walls). Based on the limited amplitude of joints deformations, in particular, friction effects were found to involve minimum variations on the actual 3D dynamic estimations, being directly related to the sliding of joints.

3.3.4. *In-plane flexible diaphragms*

The presence of an in-plane flexible diaphragm at the roof level was finally taken into account for the B01 system. In most of the cases of

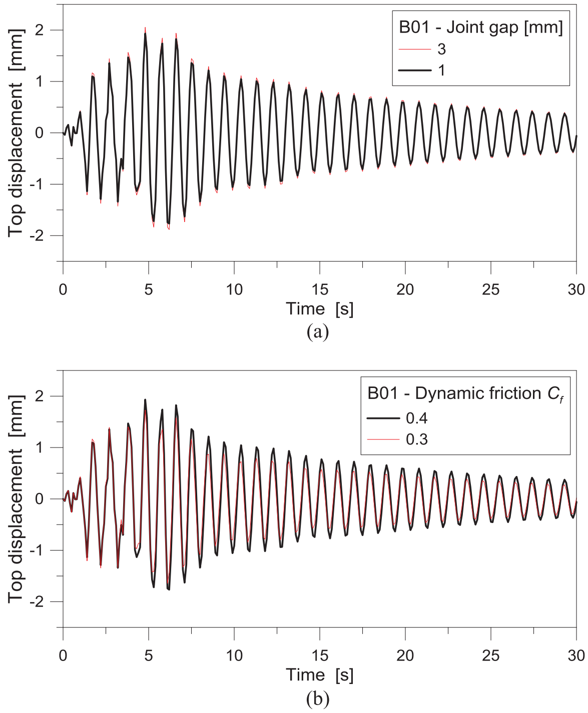

Fig. 11. Effect of (a) joint gap and (b) dynamic friction coefficient on the seismic performance of the B01 case study building (PGA = 0.35 g), in terms of time-top displacement history (ABAQUS).

practical interest for log-house structures, the typical roof and inter-storey floor are in fact expected to behave as an in-plane fully rigid diaphragm – due to the presence of OSB panels (see also [4]). Nevertheless, the possible presence of fully flexible roofs and inter-storey floors should be also investigated.

For the B01 case study, a marked increase in maximum drifts was observed after the removal of the in-plane fully rigid diaphragm.

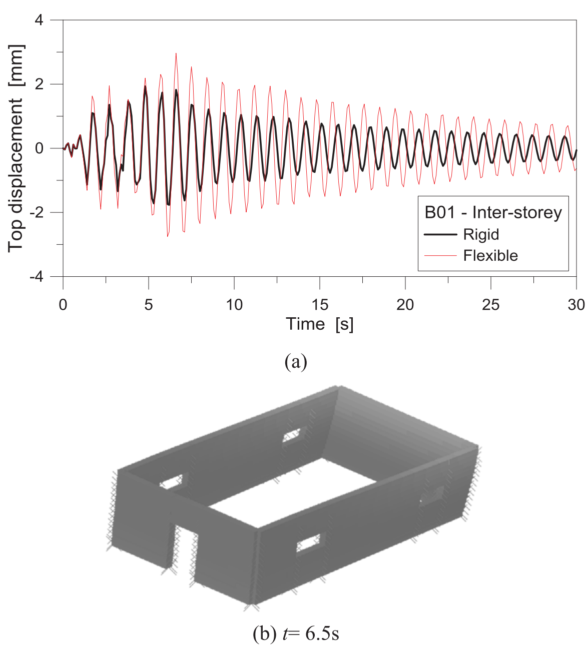

Fig. 12. Effect of in-plane fully rigid or flexible diaphragms on the seismic performance of the B01 case study building. (a) Monitored top displacement as a function of time, with (b) corresponding (extruded) 3D view for the B01 building with flexible floor (scale factor: 300, ABAQUS).

Fig. 12(a) presents a comparison of maximum drifts, as obtained from one of the seven assigned seismic records of Fig. 9(a). The corresponding deformed shape (t = 6.5 s) is also proposed in Fig. 12(b), in the form of an extruded 3D view of the building. In terms of seismic design provisions, it is thus clear that specific rules should be provided for timber log systems with flexible inter-storey floors. In the current research study, however, only in-plane fully rigid diaphragms were considered. These research outcomes should therefore be further extended.

4. q-factor estimation for log-house systems

A final exploratory investigation was carried out, in order to quantify the actual dissipative capacity and seismic resistance of timber log-wall structural systems. While in [23] single log-walls under in-plane seismic loads were considered for an estimation of the expected q-factor, in this paper full 3D buildings were analyzed, aiming to provide more reliable values.

Although a proper estimation of the q-factor is essential in the force-based design of structural systems, the current generation of design standards for timber structures [6,7] does not provide exhaustive recommendations for log-house systems and other widespread structural systems. As such, several research efforts have been spent over the last years, with careful consideration for several timber or hybrid structural systems (see for example [27–30], etc.), aiming to provide design recommendations to be implemented in standards (see also [22]).

In this paper, two different methodologies were considered for the seismic assessment of log-house systems, being characterized by different definitions of the yielding configurations for the carpentry joints in use. As shown, given the general definition of both the assumed methodologies, their reliability for log-house systems can lead to markedly different estimations.

4.1. Method 1 (M1)

Through the parametric study, nonlinear dynamic analyses (NLDA) were carried out on the B01 case study (Fig. 5(a)). The same set of seven recorded earthquake ground motions was considered as previously defined, see Fig. 9(a).

For each NLDA simulation, the magnitude of the input seismic records was sequentially increased, so that the values representative of (i) the PGA leading to a pre-fixed maximum inter-storey drift and (ii) the PGA leading to yielding could be collected. In accordance with the past exploratory FE study carried out on single walls only [23], specifically, these reference limit values were defined as:

i. $PGA_{u,i}$ (Near Collapse Limit State, NCLS): peak ground acceleration leading to a pre-fixed maximum level of inter-storey drift; and
ii. $PGA_{y,i}$ (Damage Limit State, DLS): design peak ground acceleration leading to yielding of a single corner joint.

For each *i*-scaled accelerogram, the q_0 value was then estimated as the average ratio of the so collected $PGA_{u,i}$ and $PGA_{y,i}$ peak ground accelerations, so that the corresponding q-factor value could be given by:

$$q = q_0 \cdot \gamma_M \qquad (2)$$

with γ_M the partial safety coefficient for timber [7] - namely assumed equal to 1.3 for dissipative systems - according to the proposal of revision of Section 8 for the Eurocode 8 published in [22].

4.1.1. Ultimate configuration (NCLS)

The ultimate limit for the NCLS was preliminary assumed at the attainment of a pre-fixed maximum inter-storey drift δ_{max} derived from standards. In FEMA 356 [31], for example, the NCLS damage configuration for wooden walls corresponds to a 3% transient or permanent inter-storey drift, with severe damage of the primary timber components (i.e., *"Connection loose, nails partially withdrawn; some splitting of members and panels; veneers dislodged"*).

Based on the observed structural response of single log-walls under in-plane seismic loads (see [14] for a detailed discussion of results), as well as on the shake table test results presented in [18]), a largest ultimate drift was also considered (δ_{max} = 5%). This latter NCLS configuration, although recommended in FEMA 356 [31] for steel frames only, was in fact rationally applied in this research investigation to log-house buildings, due to their intrinsic high flexibility. The choice of an higher drift limit - see also [3,23] - was suggested in this study by the typically high ductility found in the past carpentry joint and single wall tests, hence resulting in an increased flexibility, with respect to other typologies of timber structures.

4.1.2. Yielding configuration (DLS)

Careful consideration was also given to the detection of the first yielding configuration, for the assigned carpentry joints. In accordance with [22], the DLS reference configuration was considered as the first yielding for the N01 type joints, i.e. being this latter condition associated – in accordance with Table 1 – to a single joint sliding in the order of ≈ 8.6 mm. Such a displacement amplitude corresponds to a maximum drift ratio of ≈ 0.04, for the case study buildings herein investigated.

4.2. Method 2 (M2)

A further calculation approach was then considered, and the q-behaviour factor was calculated for the B01 building by taking into account the $PGA_{u,i}$ values numerically derived according to Section 4.1. The corresponding q_0 factor, based on Eq. (2), was indeed calculated by taking into account the $PGA_{y,i}$ leading the single N01 joint to shear or compressive failure mechanisms, whatever occurs first.

Based on the carpentry joint geometry displayed in Fig. 13, for seismic design purposes and in accordance with the Eurocode 5 provisions, the shear resistance of a given timber joint should be considered as the weakest among the resisting mechanisms, i.e. a pure shear failure mechanism (see Fig. 12(a)) and a compressive collapse mechanism (see Fig. 12(b)).

All the $PGA_{y,i}$ values, in the current study, were thus derived from the experimental cyclic response of the N01 reference joint (see Table 1), as the peak ground acceleration leading – for each *i*-scaled accelerogram – the first joint of the full B01 assembly to a maximum displacement corresponding to the minimum characteristic resistance load $V_{k,min}$, where:

$$V_{k,\min} = \min(V_{shear,k}, V_{c,90,k}), \tag{3}$$

with:

$$V_{shear,k} = \frac{2}{3} A_{shear} \cdot f_{k,v}, \tag{4a}$$

and

$$V_{c,90,k} = A_{comp,eff} \cdot f_{c,90,k}. \tag{4b}$$

In Eqs. (4a) and (4b), A_{shear} and $A_{comp,eff}$ denote the logs resisting surfaces emphasized in Fig. 12, while $f_{k,v}$ and $f_{c,90,k}$ represent respectively the characteristic resistance values for C24 spruce, with respect to shear and compression perpendicular to the grain stresses respectively.

4.3. Discussion of parametric FE results

As expected, the B01 building generally showed high flexibility under the assigned set seismic records, and almost a stable global behaviour. The reference methodology for the estimation of the corresponding q-factor, and its application to log-house assemblies, however, proved to have a key role on the obtained results.

4.3.1. M1 results

In terms of q-factor estimation, the main results of the exploratory study carried out in accordance with the M1 approach are proposed in Fig. 14, in terms of PGA_u (Fig. 14(a)) and q_0 values (Fig. 14(b)) calculated for each *i*-scaled accelerogram. The average values are also proposed in the form of straight lines. The so collected FE data are shown for two different NCLS scenarios (with δ_{max} = 3% and 5% respectively).

As shown, the FE results generally confirmed the preliminary findings proposed in [23] for single log-walls under in-plane seismic loads, even in presence of full 3D assemblies allowing for a box structural performance of the building. The NLDA simulations highlighted, in particular, that the assumption of a reference NCLS drift δ_{max} = 3% as conventionally done for wooden structures would result in fully neglecting the post-yielding behaviour of the adopted carpentry joints. This is also in line with earlier FE results summarized in Sections 2 and 3, and derived from the typical cyclic response of a single joint (see also Table 1 and Fig. 10(b)). As far as the carpentry joints are assumed to behave elastically under the assigned seismic records, this assumption would result in an underestimation of their actual potential, that is in a q_0-factor equal to ≈ 1 (see Fig. 14(b))and a final q-factor ≈ 1.3 (Eq. (2)).

For the B01 case study, an average q value of 1.28 at a maximum drift of 3% was in fact numerically obtained.

When the ultimate allowable drift is increased to 5%, the maximum sliding in each carpentry joint is such that they can progressively activate in the form of efficient mechanical components for the full 3D

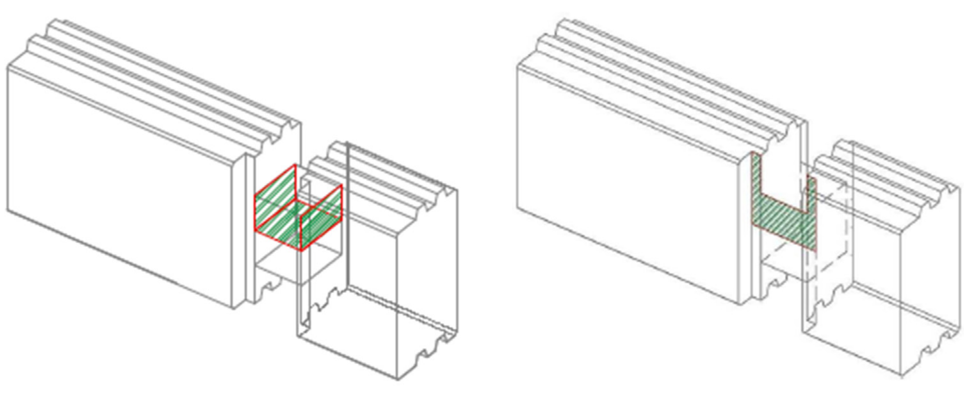

(a) (b)

Fig. 13. Reference resisting surfaces for a N01 type carpentry joint, with evidence of (a) shear or (b) compressive failure mechanisms.

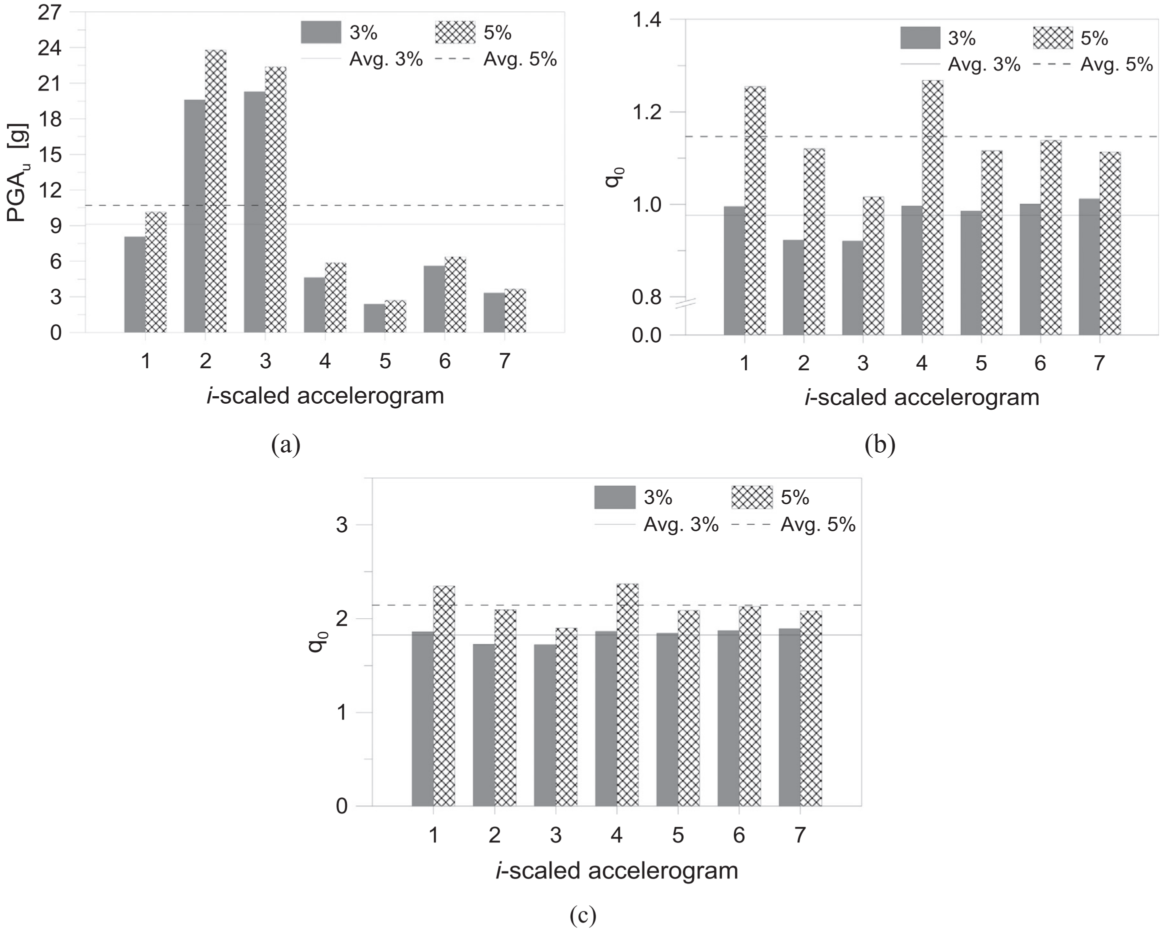

Fig. 14. q-factor estimation for the B01 case study building. (a) $PGA_{u,i}$ and (b) q_0-factor values, according to Method 1; and (c) q_0-factor values, based on Method 2 (ABAQUS).

assemblies they belong As a result - even in presence of limited deformations that each joint has to suffer, as a part of a full log-wall - the intrinsic flexibility and dissipative capacity of log-house buildings can be further exploited. In this regard, the use of a 5% maximum drift for log-house systems was proved to still result (see also Sections 2 and 3) in a typical stable performance of 3D systems under seismic records. For the examined B01 system, for example, the latter assumption numerically manifested in the form of an average q_0-factor in the order of ≈ 1.15, hence leading to a mean q-factor of ≈ 1.49 (Eq. (2)).

Due to the high deformation capacity of log-house structural systems, however, the same FE results proved that even the assumption of a 5% maximum drift does not fully exploits the potential of the adopted joints, with sliding amplitudes up to ≈ 11 mm for the reference case study.

4.3.2. M2 results

Following the M2 approach earlier proposed for the q-factor estimation, mostly different predictions were achieved compared to Section 4.3.1, see Fig. 14(c). Such an outcome is related to the actual performance of the joints in use.

For the examined N01 type joints, in particular, the shear collapse mechanism was found to be the weakest expected one, with $V_{shear,k} \approx 12$ kN the characteristic resistance derived from Eq. (3). According to the reference cyclic joint performance depicted in Table 1, a yielding displacement ≈ 4.6 mm was hence taken into account (i.e., corresponding to a maximum total drift $\approx$2%). Fro the non-linear dynamic analyses, an average q_0 value of 1.82 and 2.14 was obtained for a NCLS drift limit of 3% and 5%, see Fig. 14(c), hence resulting in a q-factor in the order of 2.4 and 2.8 (Eq. (2)) respectively, and suggesting enhanced seismic performances for the structural systems object of investigation.

More in detail, such an increase in the expected ductility capacity for the examined log-house buildings, compared to the M1-related estimations, strictly depends on the detection of the yielding configuration for the joints in use.

It should be notice, however, that the so calculated q-values are strictly related to the geometrical and mechanical features of carpentry joints in use (N01 type, in the current FE parametric study), and hence should be further assessed by taking into account a widest set of configurations of technical interest (i.e. by changing the joint properties and hence the resistance values given by (Eq. (3)), as well as by including further building configurations with more pronounced irregularities, etc.).

4.4. Derivation of design recommendations

The observations collected from the exploratory FE investigations summarized in this paper are listed herein after.

1) The FE study, in particular, confirmed the high flexibility and potential of the examined structural system under seismic loads. For the reference NCLS configuration, as also in agreement with earlier experimental and numerical studies, a maximum inter-storey drift of 5% should be considered, rather than the 3% value usually accepted for wooden structures.
2) Compared to single log-walls under in-plane lateral loads - despite the lack of mechanical interaction between stacked logs, as well as the presence of tolerance gaps in carpentry joints, or structural discontinuities in the vicinity of door/window openings - 3D full

assemblies proved to have a rather stable dynamic behaviour, due to interlocking between orthogonal walls as well as to in-plane rigid inter-storey floors.

3) The geometrical features of the typical carpentry joints currently used in log-house systems (3 joint types, in this study, with corresponding elastic stiffness, resistance and ultimate deformation) proved to have negligible effects on the overall seismic performance of the examined buildings. This finding directly depends on the presence of small gaps within the single joints, hence on their intrinsic flexibility under in-plane lateral loads and on pure contact phenomena occurring in the joints themselves.
4) Minor effects on the actual dynamic response were also observed to derive from the amplitude of tolerance gaps in joints (i.e. typically in the order of 1–3 mm) as well as from the amount of the dynamic friction coefficient, due to the global rather local behaviour of 3D log-house buildings.
5) As long as in-plane fully rigid diaphragms are considered (like in most of the modern log-house systems), a q-behaviour factor at least equal to 1.5 should be considered in design. The so calculated values, however, strictly depend on the assigned NCLS and DLS reference conditions, as well as on the geometrical and mechanical features of the joints in use. Careful consideration should be spent especially for the detection of the DLS state. When the latter condition was determined based on the shear/compressive resistance of a single carpentry joint (see M2 results), higher dissipative capacities for log-house systems and q-factors in the order of 2.4–2.8 were in fact derived from the same FE simulations, hence suggesting the need of further extended parametric analyses.
6) The presence of fully flexible diaphragms should be also properly explored, since typically resulting in a different global behaviour of the examined buildings, hence in specific q-factor values that should be properly calculated. As a result, appropriate design regulations should be provided also for the latter configuration.

5. Conclusions

The dynamic performance of log-house structural systems is typically characterized by several geometrical and mechanical aspects (i.e., cross-section features of timber logs and carpentry joints, roof-to-wall interactions, non-regular geometries, door/window openings, etc.), being mainly dependent on the intrinsic features of such systems. Current design standards for timber structures, however, do not provide accurate recommendations for log-house buildings, hence still requiring detailed investigations, especially with respect to their seismic behaviour as full 3D assemblies (i.e., global performance, local phenomena, performance parameters, etc.) or to their actual energy dissipation capacities under earthquakes (i.e., q-factor).

In this paper, in order to partly overcome these standard lacks, an exploratory nonlinear dynamic FE-investigation was proposed for full 3D log-house timber buildings. The novelty of the present study, which follows and extends past literature efforts mainly focused on the experimental and numerical seismic assessment of single components or walls, is the application of a simplified but realistic FE modelling approach to geometrically complex building systems, aiming to explore their global performance under seismic conditions, as well as to provide reliable estimations of their q-behaviour factor. The adopted FE modelling approach was first assessed towards the few experimental results of literature, as obtained from a set of full-scale shaking table tests and modal identification measurements carried out on a reference, 2-storey log-house building (i.e. the 'Rusticasa building' investigated within the past SERIES Project). In general - despite the simplified FE modelling assumptions and the influence of multiple aspects affecting the dynamic response of 3D log-house systems, as well as the uncertainty of single test repetitions - a rather good agreement was found. Parametric FE analyses were hence carried out on selected case study buildings. The so obtained results were critically discussed for some geometrical configurations of technical interest, in order to provide useful recommendations towards the calibration of specific design rules. In general - even in presence of non-regular geometrical features and multiple door/window openings - the selected buildings proved to offer a stable and markedly flexible performance under the assigned seismic records (up to PGA = 0.35 g). These numerical findings were found to mainly depend upon the key features of log-house systems, being composed of stacked logs and interacting together via carpentry joints, and namely represented by multiple contacts, gaps, friction phenomena, etc. Calculations for the q-behaviour factor were then proposed for the selected configurations, based on non-linear dynamic analyses. The discussed FE results showed that - even under severe seismic records - the single carpentry joints are mostly subjected to limited deformations, as the top displacement of a given log-house building results from the sum of progressive sliding mechanisms of the overlapping logs. This manifest in high deformation capacity and on a q-behaviour factor that can lie in the order of 2.8. Based on the so collected FE data, the parametric investigation herein discussed could hence provide a useful background for the implementation of more detailed q-factor rules and recommendations, within the next generation of seismic design standards for log-house buildings.

Acknowledgments

This research investigation was carried out within a collaboration with Rubner Haus AG SpA (www.haus.rubner.com), which is gratefully acknowledged for the financial support.

DPC-ReLUIS is also acknowledged for partially funding the research activity within the framework of the 'PR4-Timber structures' project.

A special thanks is for Mr. Daniel Gasser and Ms. Annalisa Battisti (Rubner Haus), for providing technical data and support during the experimental investigations carried out on full-scale log-house timber walls as well as on small carpentry joints. Prof. Maurizio Piazza (University of Trento, Italy) and Dr. Jorge Branco (University of Minho, Portugal) are finally also acknowledged for providing technical details on the SERIES project experiments carried out on the 'Rusticasa building'.

References

[1] Rubner Haus AG SpA, ⟨www.haus.rubner.com⟩.
[2] EN 338. Structural timber-strength classes. Brussels, Belgium: European Committee for Standardization (CEN); 2009.
[3] Bedon C, Rinaldin G, Fragiacomo M. Non-linear modelling of the in-plane seismic behaviour of timber Blockhaus log-walls. Eng Struct 2015;91:112–24.
[4] Bedon C, Rinaldin G, Izzi M, Fragiacomo M, Amadio C. Assessment of the structural stability of Blockhaus timber log-walls under in-plane compression via full-scale experiments. Constr Build Mater 2015;78:474–90.
[5] Bedon C, Fragiacomo M. Numerical and analytical assessment of the buckling behaviour of Blockhaus log-walls under in-plane compression. Eng Struct 2015;82(1):134–50.
[6] EN 1995-1-1. Eurocode 5 - Design of timber structures - Part 1-1: general-common rules and rules for buildings. Brussels, Belgium: European Committee for Standardisation (CEN); 2009.
[7] EN 1998-1. Eurocode 8 - Design of Structures for Earthquake Resistance - Part 1: general rules, seismic actions and rules for buildings. Brussels, Belgium: European Committee for Standardisation (CEN); 2004.
[8] Bedon C, Fragiacomo M. Derivation of buckling curves via FE modelling for in-plane compressed timber log-walls in accordance with the Eurocode 5. Eur J Wood Wood Prod 2016;75(3):449–65.
[9] Bedon C, Fragiacomo M. Experimental and numerical analysis of in-plane compressed unprotected log-haus timber walls in fire conditions. Fire Saf J 2018. https://doi.org/10.1016/j.firesaf.2017.12.007.
[10] Bedon C, Fragiacomo M. Fire resistance of in-plane compressed log-house timber walls with partial thermal insulation. Buildings 2018. [in print].
[11] Scott RJ, Leichti RJ, Miller TH. An experimental investigation of foundation anchorage details and base shear capacity for log buildings. For Product J 2005;55(4):38–45.
[12] Scott RJ, Leichti RJ, Miller TH. Finite-element modeling of log wall lateral force resistance. For Product J 2005;55(9):48–54.
[13] Graham DA, Carradine DM, Bender DA, Dolan JD. Performance of log shear walls subjected to monotonic and reverse-cyclic loading. J Struct Eng 2010;136(1):37–45.
[14] Branco JM, Araújo JP. Structural behaviour of log timber walls under lateral in-

plane loads. Eng Struct 2012;40(3):371–82.
[15] Bedon C, Fragiacomo M, Amadio C, Sadoch C. Experimental study and numerical investigation of Blockhaus shear walls subjected to in-plane seismic loads. J Struct Eng 2015;141(4). https://doi.org/10.1061/(ASCE)ST.1943-541X.0001065. [article number 04014118].
[16] Grossi P, Sartori T, Giongo I, Tomasi R. Analysis of timber log-house construction system via experimental testing and analytical modelling. Constr Build Mater 2016;102(2):1127–44.
[17] Sciomenta M, Bedon C, Fragiacomo M, Luongo A. Shear performance assessment of timber log-house walls under in-plane lateral loads via numerical and analytical modelling. Buildings 2018;8(8):99. https://doi.org/10.3390/buildings8080099.
[18] Piazza M, Tomasi R. Investigation of seismic performance of multi-storey timber buildings within the framework of the SERIES Project. Proceedings of the 2nd International Conference on Structures and Architecture – ICSA, Portugal, 2013, pp. 82–89.
[19] Piazza M. Seismic performance of multi-storey timber buildings – Rusticasa building – Final Report, SERIES 227887 Timber Buildings Project; 2013.
[20] Branco JM, Lourenço PB, Aranha CA. Seismic analysis of a 2-storey log house. Adv Mater Res 2013;778:478–85.
[21] Buchanan A, Moroder D. Log house performance in the 2016 Kaikoura earthquake. Bull NZ Soc Earthq Eng 2017;50(2):225–36.
[22] Follesa M, Fragiacomo M, Vassallo D, Piazza M, Tomasi R, Rossi S, Casagrande D. A proposal for a new Background Document of Chapter 8 of Eurocode 8, Proceedings of INTER 2015 Meeting Šibenik, Croatia, Paper n 48-7-3; 2015.
[23] Bedon C, Rinaldin G, Fragiacomo M, Amadio C. Exploratory cyclic and dynamic numerical investigation for the assessment of the seismic vulnerability of Blockhaus shear walls under in-plane lateral loads. Proceedings of XVI ANIDIS Conference, 13-17September, L'Aquila, Italy; 2015.
[24] Rinaldin G, Amadio C, Fragiacomo M. A component approach for the hysteretic behaviour of connections in cross-laminated wooden structures. Earthq Eng Struct Dyn 2013;42(13):2023–42. https://doi.org/10.1002/eqe.2310.
[25] Simulia. ABAQUS v.6.12 [Computer Software], Dassault Systems, Providence, RI, USA; 2012.
[26] Iervolino I, Galasso C, Cosenza E. REXEL: computer aided record selection for code-based seismic structural analysis. Bull Earthq Eng 2010;8(2):339–62. https://doi.org/10.1007/s10518-009-9146-1.
[27] Ceccotti A, Sandhaas C. A proposal for a standard procedure to establish the seismic behaviour factor q of timber buildings. Proceedings of WCTE 2010 – World Conference on Timber Engineering, Riva del Garda, Italy, 2010, pp. 3604–3614, paper code 94027.
[28] Pozza L, Scotta R, Trutalli D, Polastri A, Smith I. Experimentally based q-factor estimation of cross-laminated timber walls. Struct Build 2016;169(7):492–507.
[29] Chen Z, Chui YH, Doudak G. An approach for estimating seismic force modification factor of hybrid building systems. Proceedings of WCTE 2014 – World Conference on Timber Engineering, Quebec City, Canada, paper code 110957; 2014.
[30] Zhang Z, Fairhurst M, Tannert T. Ductility estimation for a novel timber-steel hybrid system. J Struct Eng 2016;142(4). https://doi.org/10.1061/(ASCE)ST.1943-541X.0001296#sthash.I7RxLdy5.dpuf.
[31] FEMA 356. Prestandard and commentary for the seismic rehabilitation of buildings. Washington, DC: Federal Emergency Management Agency; 2000.